

RI 9393

**RI 9393**

REPORT OF INVESTIGATIONS/1991

*e. 1 of 2*  
**For Reference**  
*Library*

**Not to be taken from this room**

LIBRARY  
SPOKANE REGIONAL  
UNIVERSITY

JAN 1992

U.S. DEPARTMENT OF THE INTERIOR  
BUREAU OF MINES  
SPOKANE REGIONAL

# Characteristics of Mining-Induced Seismicity and Rock Bursting in a Deep Hard-Rock Mine

By P. L. Swanson and C. D. Sines

UNITED STATES DEPARTMENT OF THE INTERIOR



BUREAU OF MINES

**Mission:** As the Nation's principal conservation agency, the Department of the Interior has responsibility for most of our nationally-owned public lands and natural and cultural resources. This includes fostering wise use of our land and water resources, protecting our fish and wildlife, preserving the environmental and cultural values of our national parks and historical places, and providing for the enjoyment of life through outdoor recreation. The Department assesses our energy and mineral resources and works to assure that their development is in the best interests of all our people. The Department also promotes the goals of the Take Pride in America campaign by encouraging stewardship and citizen responsibility for the public lands and promoting citizen participation in their care. The Department also has a major responsibility for American Indian reservation communities and for people who live in Island Territories under U.S. Administration.

**Report of Investigations 9393**

**Characteristics of Mining-Induced  
Seismicity and Rock Bursting  
in a Deep Hard-Rock Mine**

**By P. L. Swanson and C. D. Sines**

**UNITED STATES DEPARTMENT OF THE INTERIOR  
Manuel Lujan, Jr., Secretary**

**BUREAU OF MINES  
T S Ary, Director**

**Library of Congress Cataloging in Publication Data:**

**Swanson, P. L. (Peter L.)**

Characteristics of mining-induced seismicity and rock bursting in a deep hard-rock mine / by P.L. Swanson and C.D. Sines.

p. cm. — (Report of investigations; 9393)

Includes bibliographical references (p. 12).

Supt. of Docs. no.: I 28.22:9393.

1. Rock bursts—Idaho—Coeur d'Alene Region—Measurement. 2. Microseisms—Idaho—Coeur d'Alene Region—Measurement. I. Sines, Clinton D. II. Title. III. Series: Report of investigations (United States. Bureau of Mines); 9393.

TN23.U43

[TN317]

622' .28—dc20

91-26202

CIP

## CONTENTS

	<i>Page</i>
Abstract .....	1
Introduction .....	2
Instrumentation .....	2
Surface seismograph .....	2
Microseismicity monitoring system .....	2
Seismic event location method .....	2
Magnitude scale .....	4
Results .....	5
Discussion .....	10
Summary .....	11
References .....	12

## ILLUSTRATIONS

1. Mining-induced seismic activity .....	3
2. Use of microseismicity to constrain seismic event location .....	4
3. Empirical relation between logarithm of seismic signal duration and seismic magnitude .....	5
4. Seismic magnitude versus time of occurrence .....	6
5. Seismic energy release during study period .....	7
6. Histogram of magnitudes for surface-recorded events located during study period .....	7
7. Logarithm of number of seismic events .....	7
8. Histogram of occurrence times for located seismic events .....	8
9. Histogram of occurrence times for damaging rock bursts .....	8
10. Distribution of event magnitudes for damaging rock bursts throughout mine .....	9
11. Distribution of event magnitudes for damaging and minor rock bursts occurring near single stope .....	9
12. Histogram of occurrence times for damaging and minor rock bursts in single stope .....	10
13. Estimates of characteristic source dimensions .....	11

### UNIT OF MEASURE ABBREVIATIONS USED IN THIS REPORT

Hz	hertz	m <sup>3</sup>	cubic meter
h	hour	min	minute
J	joule	pet	percent
km	kilometer	s	second
lb	pound	V/g	volt per acceleration
m	meter		

### SYMBOLS USED IN THIS REPORT

a <sub>1</sub> , a <sub>2</sub> , a <sub>3</sub>	constants used to derive M	M	local Richter magnitude
b	slope of the logarithm of the number of events with magnitude greater than M versus M	N	number of seismic events
E	seismic energy	Ω	frequency-dependent seismic displacement
f <sub>c</sub>	corner frequency	R	hypocentral distance, km
g	gravity constant	T	coda duration, s
		V	source volume

# CHARACTERISTICS OF MINING-INDUCED SEISMICITY AND ROCK BURSTING IN A DEEP HARD-ROCK MINE

By P. L. Swanson<sup>1</sup> and C. D. Sines<sup>2</sup>

---

## ABSTRACT

Over a recent 20-month observation period, the U.S. Bureau of Mines obtained seismogram records from a single vertical-component, short-period seismometer installed at the surface of a metal mine in northern Idaho. The seismic events were analyzed for local (Richter) magnitude ( $M$ ), time of occurrence, location, and relation to rock bursting and production blasting. Approximately 150 seismic events with  $-0.5 \leq M \leq 2.9$  were located within the mine, yielding a  $b$  value (slope of the logarithm of the number of events with magnitude greater than  $M$  versus  $M$ ) of 0.5. Event locations were constrained using a dense underground array of high-frequency accelerometers. Twenty of the surface-recorded events, with  $0.5 \leq M \leq 2.9$ , were associated with rock bursts that produced damage requiring at least 1/2 day of cleanup and/or repair. Other possibly hazardous rock bursts, with magnitudes as small as -1.1, were numerous but were not associated with significant structural damage. Approximately 60 pct of the seismic events with  $M > -0.5$  and 75 pct of damaging rock bursts occurred within 45 min of blasting. Estimates of characteristic rupture dimensions for rock bursts with  $-1.1 \leq M \leq 2.9$ , based on a conventional dislocation shear-slip model of failure, range from 3 to 300 m.

---

<sup>1</sup>Geophysicist.

<sup>2</sup>Engineering technician.

Denver Research Center, U.S. Bureau of Mines, Denver, CO.

## INTRODUCTION

One goal of the U.S. Bureau of Mines is to improve safety in the mining industry. As part of its effort to develop methods for mitigating rock burst hazards, the U.S. Bureau of Mines operates underground microseismic arrays in lead-zinc-silver mines of the Coeur d'Alene mining district of northern Idaho. In the Galena Mine (Wallace, ID), the Bureau and ASARCO Incorporated, jointly operate an extensive array of high-frequency accelerometers that is designed to provide real-time location and display of microseismic events with local (Richter) magnitudes as low as approximately -5 (1).<sup>3</sup> This experimental system is used to determine the effectiveness of real-time empirical analyses of temporal and spatial trends of microseismicity in identifying developing rock-mass instabilities. This system was designed to function as an industrial monitoring tool and was not intended to capture full waveforms for use in locating and characterizing large

seismic events and rock bursts. Quantitative characterization of these large events is necessary to develop a better understanding of rock burst mechanisms so that improvements can be made in rock burst prediction and control strategies. The present study of mining-induced seismicity was undertaken to provide basic data, such as event magnitudes and frequency of occurrence, needed to design a full waveform seismic array for characterizing source parameters of these larger events. Similar basic seismic data for rock burst-prone mines in the Republic of South Africa can be found in papers by Cook (2), Hodgson (3), McGarr (4), and Lenhardt (5-6).

The instrumentation, the method of locating the events, and the development of a local magnitude scale are first described, and then the seismic and rock burst data are presented and discussed.

## INSTRUMENTATION

### SURFACE SEISMOGRAPH

The surface seismograph sensor is a high-sensitivity, short-period, vertical-component velocity gauge. It is located on a hard-rock site under 120 m of overburden and is approximately 1.3 km above the seismic activity. Its output is band-pass filtered from 0.2 to 50 Hz, amplified, and recorded on a paper drum recorder located in the mining engineering office. The amplification at the drum recorder is adjusted so that ordinary production blasting is just perceptible above the seismic noise background. As a result, few teleseismic events are well recorded. Mining-induced events with magnitude  $\sim 1$  or greater result in waveform clipping (truncation caused by hardware limitations).

### MICROSEISMICITY MONITORING SYSTEM

The microseismicity monitoring system is described in detail in reference 1. Approximately 130 high-frequency accelerometers are distributed in 8 clusters (arrays) for monitoring 10 working areas possessing rock bursting

potential. Another 10 areas are mined but not monitored directly. The accelerometer frequency response extends to several kilohertz with a sensitivity of 40 V/g. In each cluster, remote hardware circuitry is used to measure signal arrival times, or times when threshold voltage is exceeded, on each channel. This information is transmitted to computers in an underground central recording site. Maximum event detection rate is three events per second. Approximately 10 pct of the detected events are located with acceptable quality for routine monitoring purposes; event quality is determined using various criteria during postlocation processing. In individual stopes, daily counts of located microseismic events range from several tens to 2,000, with 100 to 200 per day typical. Seismic magnitudes are not determined with this microseismicity network; most stations clip with  $M \geq -2$  events. However, relative event size is estimated by examining the number of accelerometers exceeding the threshold voltage on separate banks of high- and low-gain amplifiers. In addition, on a few channels in each cluster, signals are squared and summed for a rough measure of relative event size.

## SEISMIC EVENT LOCATION METHOD

Approximately 150 of the seismic events recorded on the surface with  $M > -0.5$  were located within 1 of

approximately 20 working areas in the mine. Figure 1 shows the number of located events plotted as a function of time. In addition to these events, a similar number of

<sup>3</sup>Italic numbers in parentheses refer to items in the list of references at the end of this report.

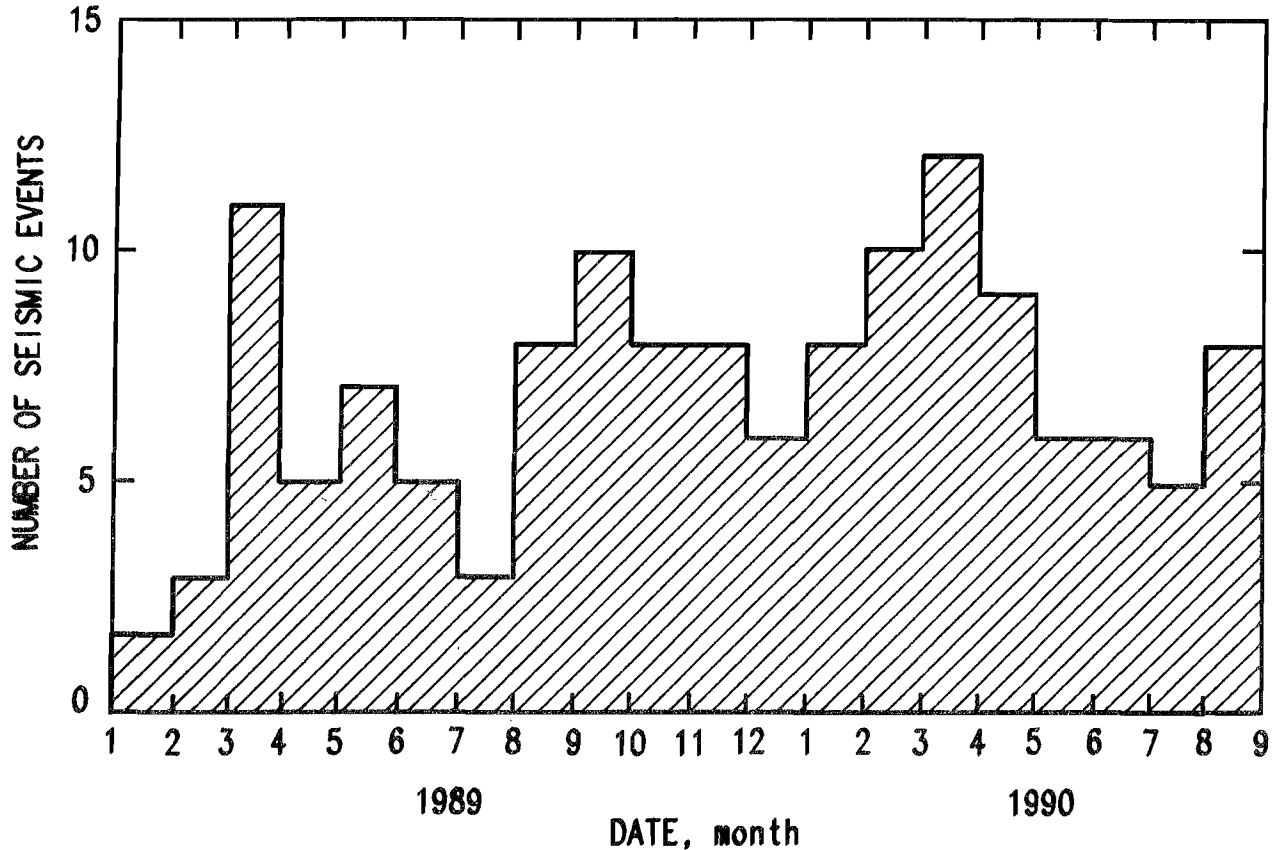


Figure 1.—Mining-induced seismic activity with magnitude  $> -0.5$  (January 1989 through August 1990).

events were recorded but not located. These were either associated with another mine in the Coeur d'Alene district or were within the vicinity of the Galena Mine but were not locatable. The analysis is restricted to those events with  $M > -0.5$  that were located within a specific working area of the mine. Three methods were used to locate seismic events recorded on the surface.

1. In the case of damaging rock bursts, the stope nearest the damage was taken as the approximate seismic source location.

2. During nonblast times, when microseismicity is not typically at a peak, microseismic activity occurring in a time window of a few minutes before and after the time of the event recorded on the surface usually indicates which stope is active. For example, the plan view maps in figure 2 show microseismic event locations in four stopes over a 10-min time interval centered on the time of a mid-day seismic event of  $M \sim 1.2$ . All monitored stopes (four

shown in figure 2, six not shown) except stope *A* in the figure display similar low to zero activity.

3. When microseismic activity is high (for example, immediately following simultaneous blasting in several working areas), the raw data from the microseismicity monitoring system must be scrutinized carefully. Although the surface seismograph and the underground microseismicity monitoring system did not share the same time base during the study period, the separate time bases were synchronized to within several seconds. Event times on the surface seismograph are resolved to 1 s, and seismic-wave travel times to the surface from the source regions (and the underground accelerometer arrays) are approximately 0.2 to 0.3 s. If occurrence times for high-energy events recorded on the microseismicity monitoring system can be correlated with the time of the surface-recorded event, a location can be established. This location method requires, of course, that the events occur within the range of one of the underground arrays.

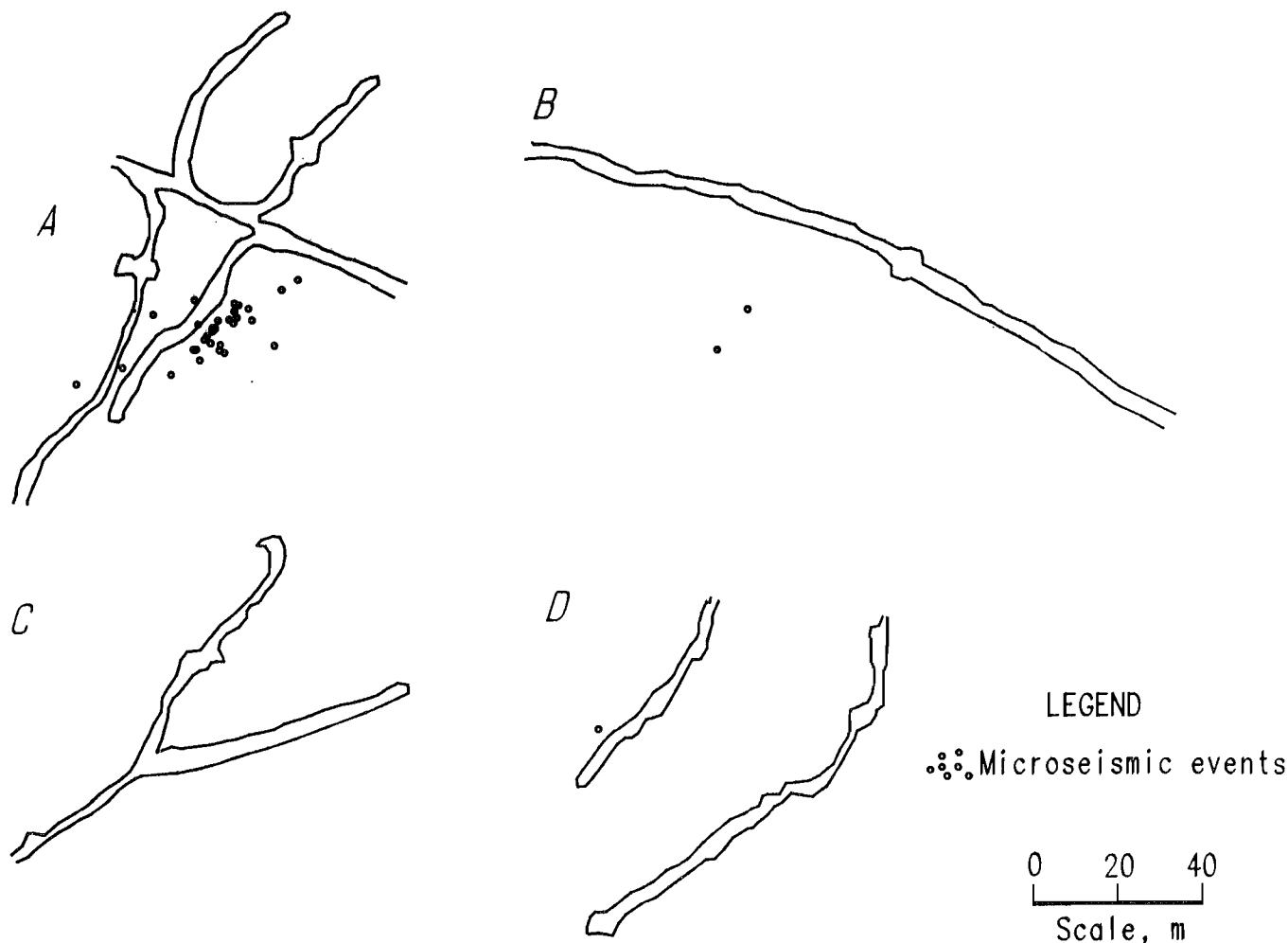


Figure 2.—Use of microseismicity to constrain seismic event location. Event locations from four (A, B, C, D) of ten monitored stopes are shown for 10-min interval encompassing time of a seismic event with magnitude of 1.2.

## MAGNITUDE SCALE

An empirical magnitude scale was established using seismic coda (signal) duration. The duration of the seismic signals was measured on the paper records and paired with event magnitudes reported by the National Earthquake Information Service and/or the Montana Bureau of Mines and Geology. Events with  $M > 2.3$  from the Galena Mine and from other nearby mines were used in the calibration. One smaller event ( $M \sim 1.2$ ) was also recorded by a nearby temporary portable network operated jointly by the Montana Bureau of Mines and Geology and the University of Idaho and was used in the calibration.<sup>4</sup> The data (fig. 3) were fit to an equation of the form

$$M = (a_1 \cdot \log[T]) + (a_2 \cdot R) + a_3, \quad (1)$$

where  $M$  is local magnitude;  $T$  is coda duration in seconds;  $R$  is hypocentral distance in kilometers; and  $a_1$ ,  $a_2$ , and  $a_3$  are constants. At the 97-pct confidence level, the constants are  $a_1 = 1.90526 \pm 0.51369$ ,  $a_2 = 0.00000 \pm 0.00003$ , and  $a_3 = -0.54216 \pm 0.00003$ . Over the applicable range of  $R$  values, this effectively reduces to

$$M = (1.9 \cdot \log[T]) - 0.5. \quad (2)$$

This calibration equation provides only a rough magnitude estimate; more precise estimates in the future may be based upon direct energy and/or coda measurements from on-scale (unclipped) digital waveforms.

<sup>4</sup>The U.S. Geological Survey seismic station at Newport, WA, was not in operation during the study period.

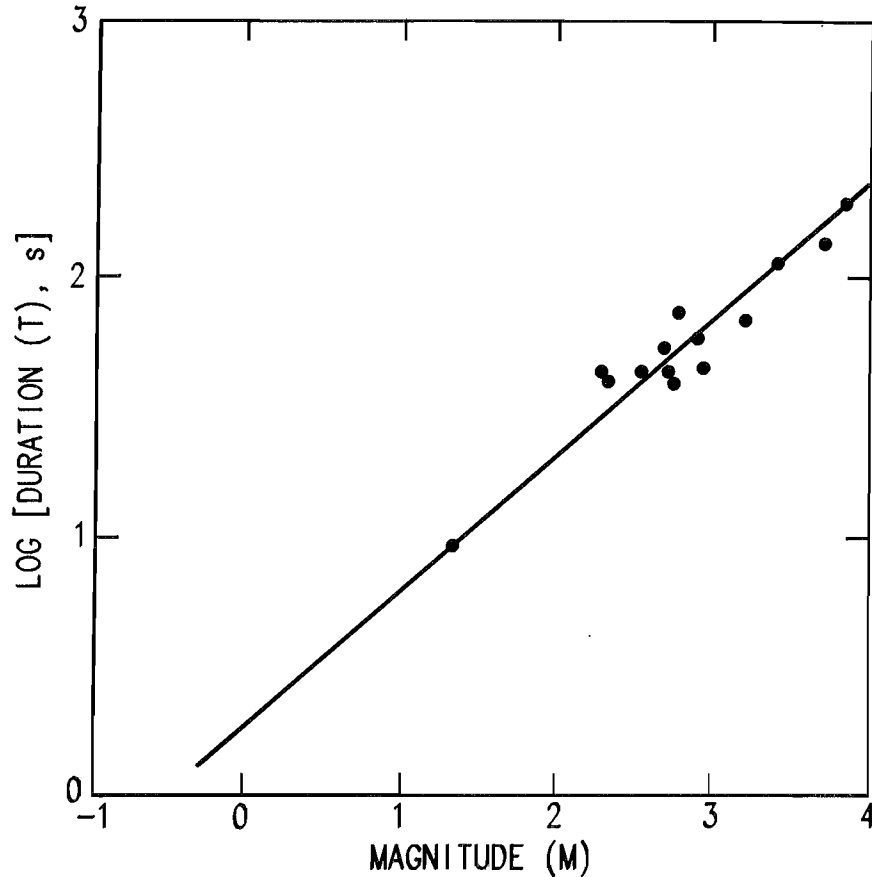


Figure 3.—Empirical relation between logarithm of seismic signal duration (T) and seismic magnitude (M).

## RESULTS

The seismic data are first presented without regard to whether they are associated with rock bursts. Subsequently, this special subset, seismic events associated with rock bursts, will be addressed.

Figure 4 shows the magnitude and occurrence time of seismic events ( $M > 0$ ) located during the 20-month observation period. While mining activity was generally constant during this period (an exception is the June 25 to July 8, 1990, shutdown), the occurrence rate of surface-recorded seismic events was varied. Throughout the study period, several stopes remained in what is known as a critical geometry for rock bursting (7), where the stope is more than 70 pct extracted. There are notable periods of low seismic activity and high activity.

Figure 5 shows the cumulative seismic energy released during this period (seismic energy is derived in equation 5). Ninety percent of the seismic energy was released in only 5 pct (eight) of the events. Of these high-energy events, half did not produce significant rock burst damage.

A histogram of the event magnitudes is shown in figure 6. In figure 7, these data, which represent events located throughout the mine, are fit to the empirical relation (8)

$$\log(N) = a - (b \cdot M), \quad (3)$$

where  $N$  is the number of events with magnitude  $M$  or greater and  $b$  is the slope of the logarithm of the number of events with magnitude greater than  $M$  versus  $M$ . The value of  $b$  in this magnitude distribution has been suggested to be related to fractal dimension (9), indicating that the size distribution is self-similar. The straight-line fit shown for data with  $M \geq 1$  yields  $b = 0.5$  and  $a = 2.3$  (the data set for  $M < 0.5$  is incomplete). At the present time, the data set is too small to obtain meaningful  $b$  values for individual working areas. The  $b$  values for natural earthquakes (10), laboratory rock fracture experiments (11-12), and mining-induced seismicity (3-4) typically range

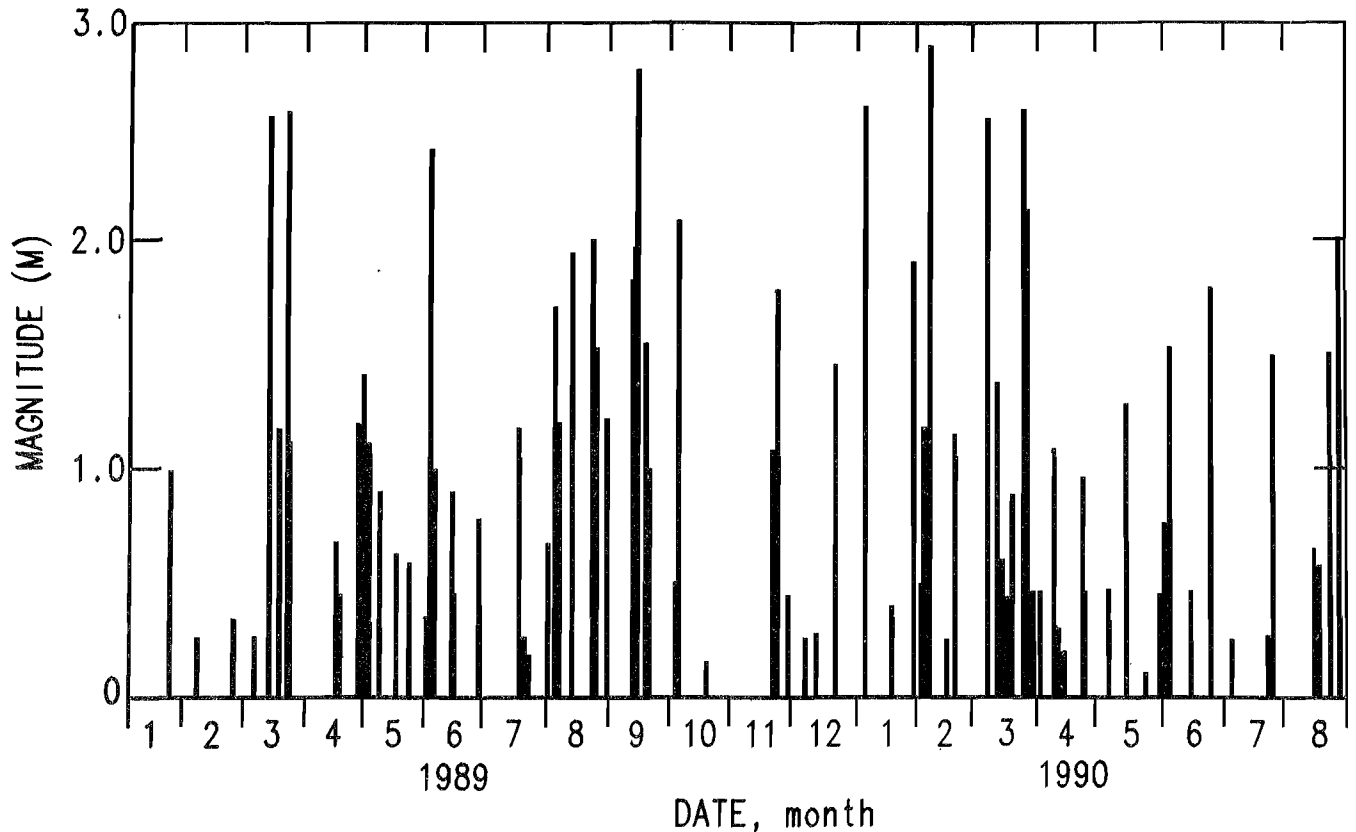


Figure 4.—Seismic magnitude versus time of occurrence for events with magnitude  $> 0$ .

from 0.5 to 1.3. Smaller  $b$  values, which indicate an enrichment of higher magnitude events, are suggestive of higher stress regimes (12) in controlled laboratory experiments. Also,  $b$  values have been observed to change as a function of time and space in the earthquake process (13).

In one study of mining-induced seismicity, McGarr (4) observed that  $a$  in equation 3 is a function of mining geometry, but  $b$  is not measurably affected. Legge (14) observed a change in both  $a$  and  $b$  during the mining of a remnant pillar. Lenhardt (5) observed only a slight difference in  $b$  values for microseismic events associated with blasting (0.80) and events occurring during nonblast times (0.74). As attenuation can affect magnitude estimation, changing  $b$  values may be attributable to ray path effects as well as source effects.

The direct relationship between seismic activity and mining activity is immediately apparent from figure 8, which shows the number of seismic events occurring during each of the hours of the day. Regular production

blasting takes place at approximately 14:15 and 22:15, coincident with the two peaks of activity. Sixty percent of the events with  $M > -0.5$  occurred during the 45-min period immediately following blasting (45 min chosen only for convenience).

Consideration is now given to how rock bursts are distributed throughout the day. First, a distinction is made between two kinds of rock bursts: those that produce significant damage to mine structures and those that do not. The distinction is made, as will be discussed later, to assure completeness of the data set. A damaging rock burst is arbitrarily defined, for purposes of the present discussion, as one that requires a minimum of 1/2 day of cleanup and/or repair time. The remaining minor rock bursts require less than 1/2 day of cleanup and/or repair, but may nonetheless be just as hazardous to exposed mine personnel as damaging rock bursts.

Figure 9 shows the hourly distribution of damaging rock bursts occurring throughout the mine during the study period. Seventy-five percent occurred during the 45-min

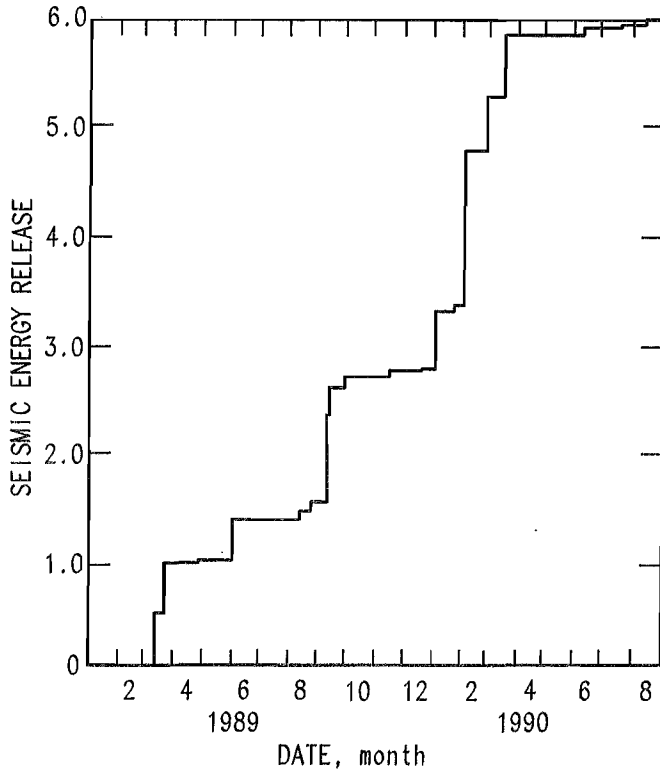


Figure 5.—Seismic energy release during study period.

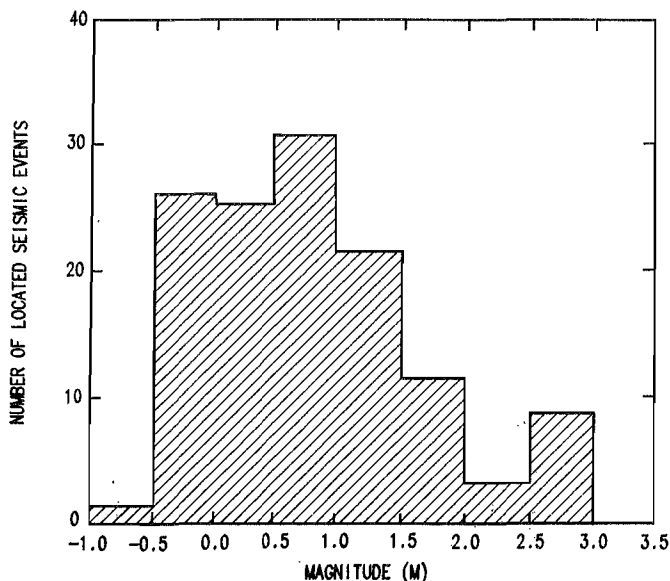


Figure 6.—Histogram of magnitudes for surface-recorded events located during study period.

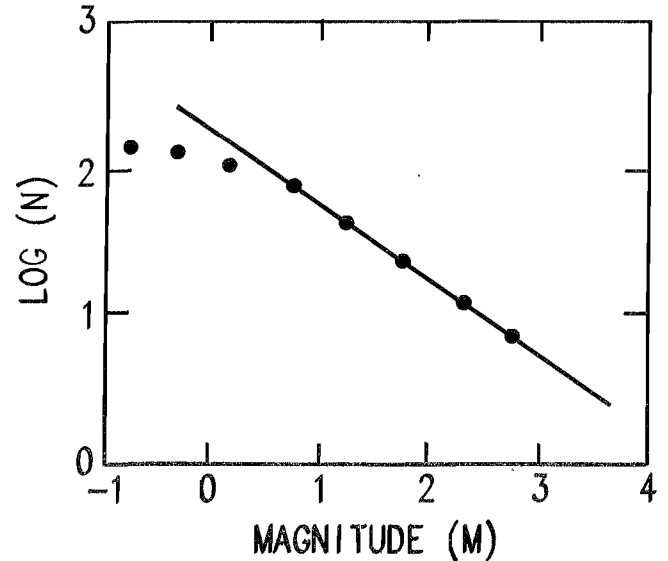


Figure 7.—Logarithm of number of seismic events with magnitude greater than  $M$ . Straight line fit to data with  $M > 0.5$  gives  $b$  value of 0.5.

period immediately following production blasting—a time when the mining areas are evacuated for blasting and shift changes. The distribution of seismic event magnitudes associated with the damaging bursts is shown in figure 10. As expected, damaging rock bursts are associated with the larger seismic events (compare with figure 6). In this particular data set, a peak exists at magnitudes between 2.5 and 3.0. However, it should be emphasized that large seismic events ( $2 < M < 3$ ) do occur without any significant damage.

Because the damaging events are not overlooked by mine personnel, they form a rather complete data set. This is not the case for the smaller magnitude minor rock bursts. With the present surface seismic system, some of these smaller events are not recorded on the surface, and when they are, it may not be possible to locate them. Or, since mine damage is minimal, they may go unnoticed or unreported. Consequently, it has not yet been possible to obtain a complete data set for the minor rock bursts occurring throughout the mine.

A fairly complete data set was obtained for one stope<sup>5</sup> that was closely monitored with a variety of instrumentation. The distribution of event magnitudes for all rock

<sup>5</sup>The sill pillar in this stope was subjected to three destress blasts during the study interval.

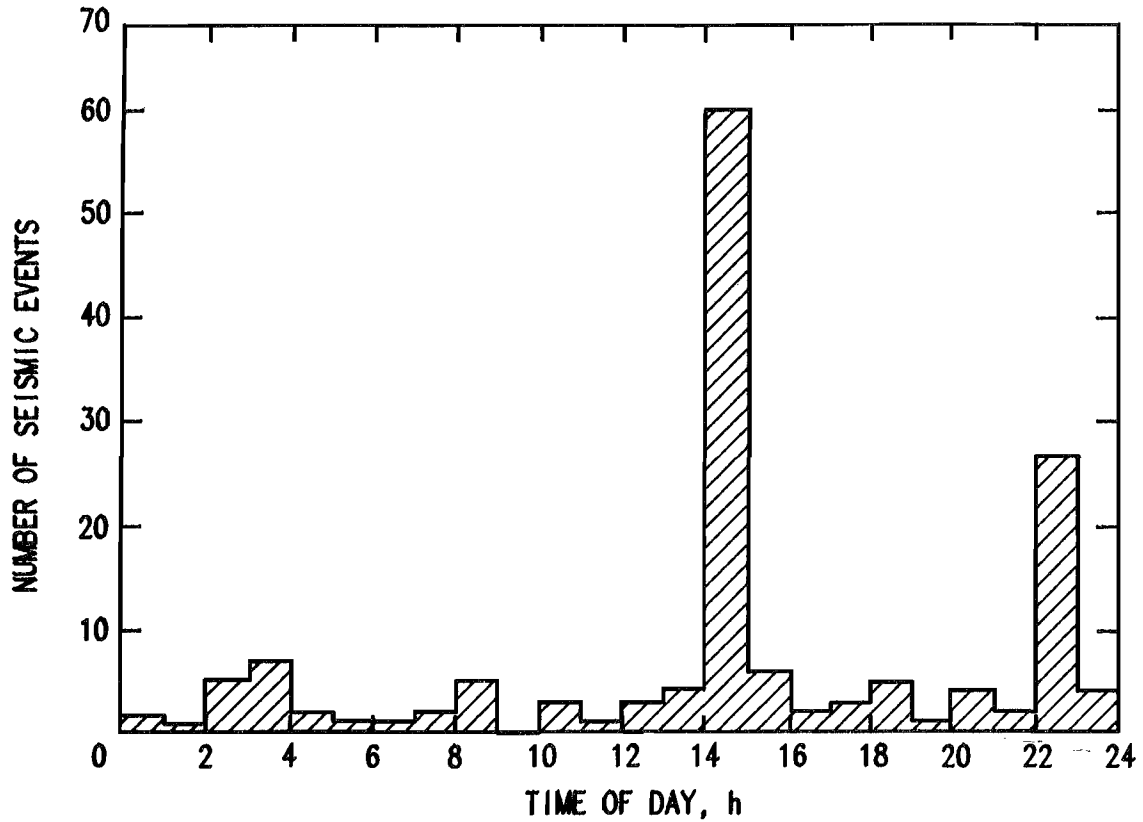


Figure 8.—Histogram of occurrence times for located seismic events with magnitude  $> -0.5$ .

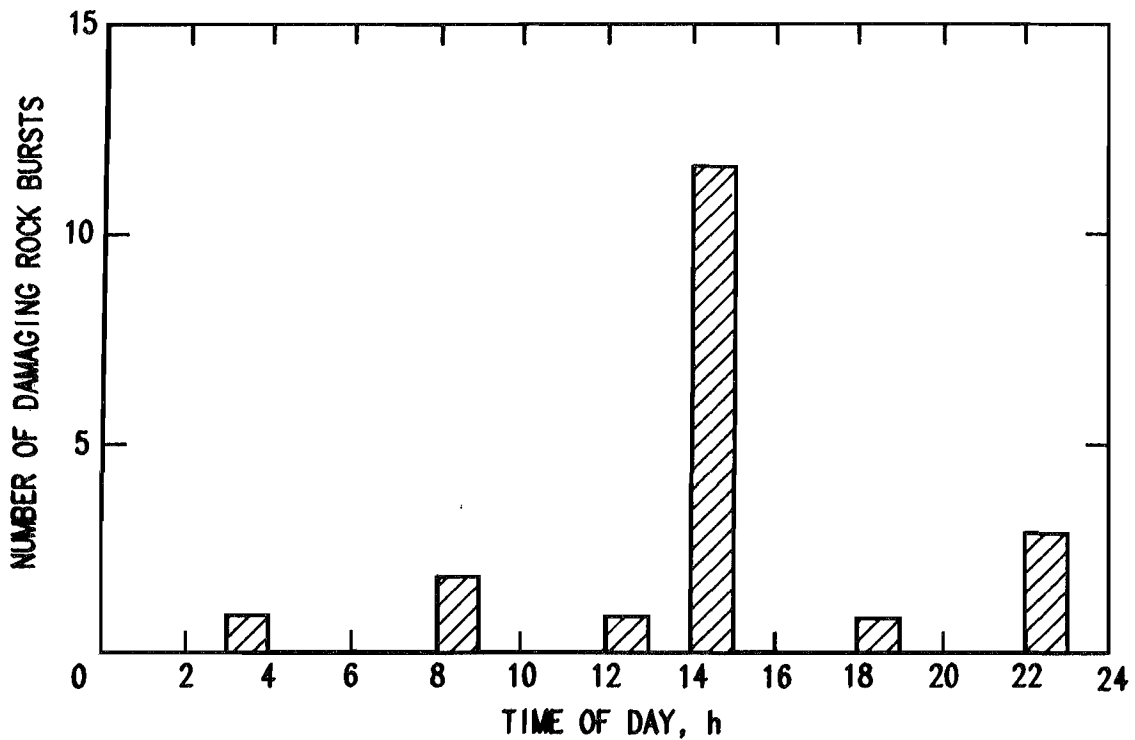


Figure 9.—Histogram of occurrence times for damaging rock bursts with magnitude  $> 0.5$ .

bursts (both damaging and minor) in the vicinity of this stope is shown in figure 11. The three damaging rock bursts in this figure had magnitudes of 0.9, 2.2, and 2.9.

The hourly distribution of the events is shown in figure 12. Forty-six percent of these events occurred in the 45-min period immediately following blasting.

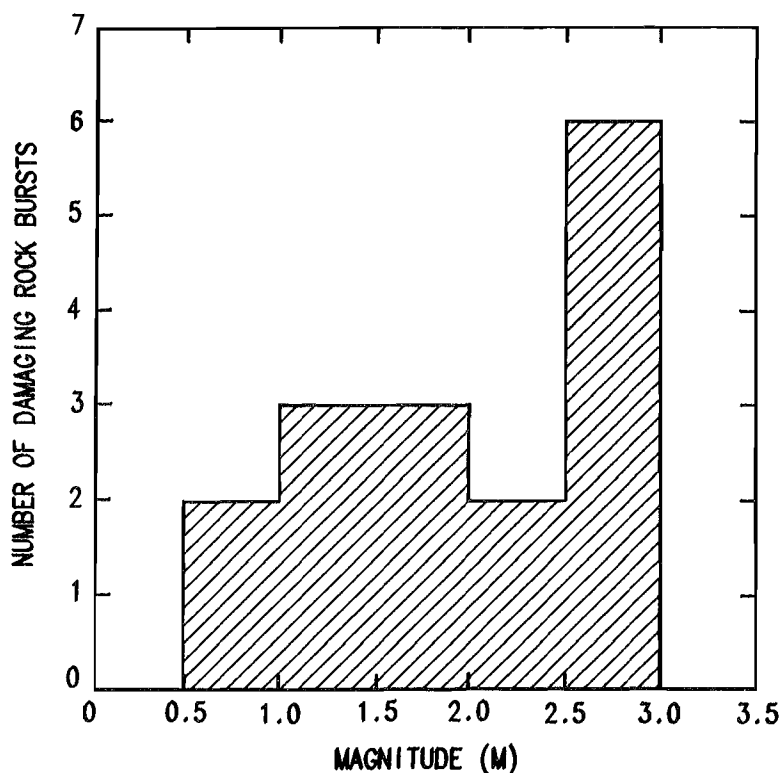


Figure 10.—Distribution of event magnitudes for damaging rock bursts throughout mine.

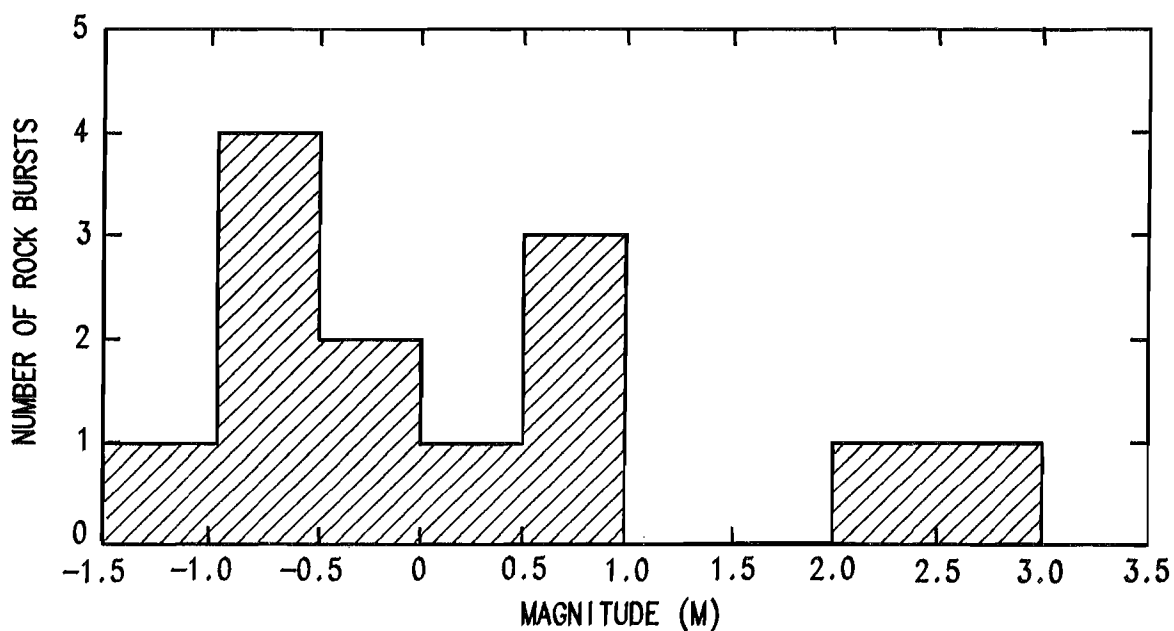


Figure 11.—Distribution of event magnitudes for damaging and minor rock bursts occurring near single stope.

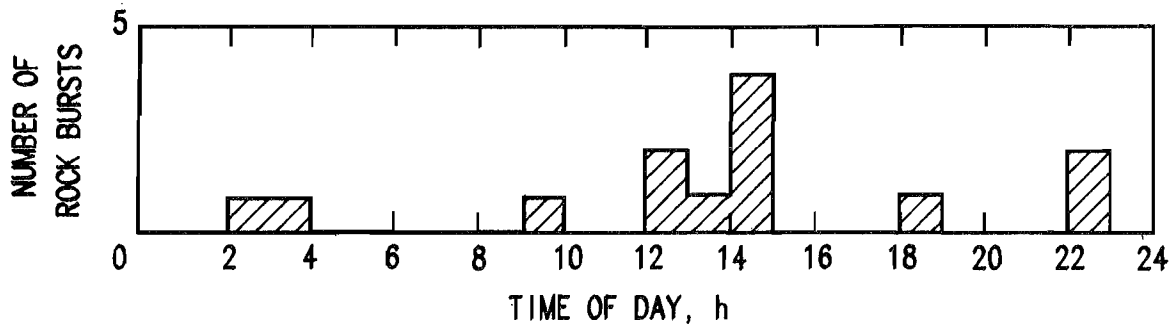


Figure 12.—Histogram of occurrence times for damaging and minor rock bursts in single stope.

## DISCUSSION

The span in size between the largest (2.9) and smallest (-1.1) rock burst is considerable. Recognition of this enormous size scale variation leads to an appreciation of the difficulty in developing solutions to the problem of rock burst prediction and control. This is perhaps most obvious when considering the seismic energies and source volumes associated with this range of event magnitudes. The empirical seismic energy (E)-magnitude law found in Gutenberg (15) is introduced,

$$\log (E) = 11.8 + (1.5 \cdot M), \quad (4)$$

which was originally established for natural earthquakes. Energy E is measured in ergs ( $1 \text{ erg} = 10^{-7} \text{ J}$ ). Equation 4 has been shown to be consistent with energy and magnitude estimates for mining-induced seismicity (16). The rock bursts with magnitudes of 2.9 to -1.1 are associated with energies of  $1.4 \times 10^9$  and  $1.4 \times 10^3 \text{ J}$ , respectively, or a factor of  $10^6$  variation. For comparison, the seismic energy released by 1 lb of dynamite is approximately  $1.4 \times 10^3 \text{ J}$  (2).

A characteristic source dimension is estimated in two ways. First, the source volume is taken to be a sphere centered on the seismic source. The source volume is considered to represent the volume from which a major portion of the radiated elastic energy is derived. Combining equation 4 with an empirical relation between seismic magnitude and area of disturbed surface features for shallow earthquakes, a relation between source volume V and seismic energy can be derived (17),

$$\log (E) = \log (V) + 3.0. \quad (5)$$

Applying equation 5 to the largest and smallest rock bursts yields  $V = 2.41 \times 10^7$  and  $14.1 \text{ m}^3$ , respectively, with corresponding source radii of 150 and 1.5 m, respectively.

With the second method, source radii are obtained from independent estimates of rupture dimensions from magnitude and rupture-size relations based on Brune's seismic source model (18-19). This model predicts that a dislocation shear-slip type of dynamic rupture will result in far-field seismic waveform spectra that can be characterized by two asymptotes described by  $\Omega_0$  and  $f_c$ . The flat, low-frequency portion of the seismic displacement spectrum,  $\Omega_0$ , is proportional to the strength of the event or seismic moment. The corner frequency,  $f_c$ , marks the frequency at which the spectrum falls off to lower values, and  $f_c$  is proportional to the rupture dimension. Figure 13 summarizes estimates of seismic source radii based on this type of analysis. The data shown are primarily from studies of mining-induced seismicity in coal and hard-rock mines. For a given magnitude (or seismic moment), the source size scales inversely with stress drop across the rupture, leading to the variation shown in figure 13. Within this variation, these data support rupture dimension estimates for the largest events that are consistent with estimates from equation 5.

It is interesting to note that the inferred rupture dimensions of the largest and smallest rock bursts in the Galena Mine are roughly characteristic of interstope distances and/or intervein dimensions on the large end of the estimate and of the working face dimensions on the small end. This observation indicates the potential for the largest seismic and rock burst events to interact with adjacent stopes.

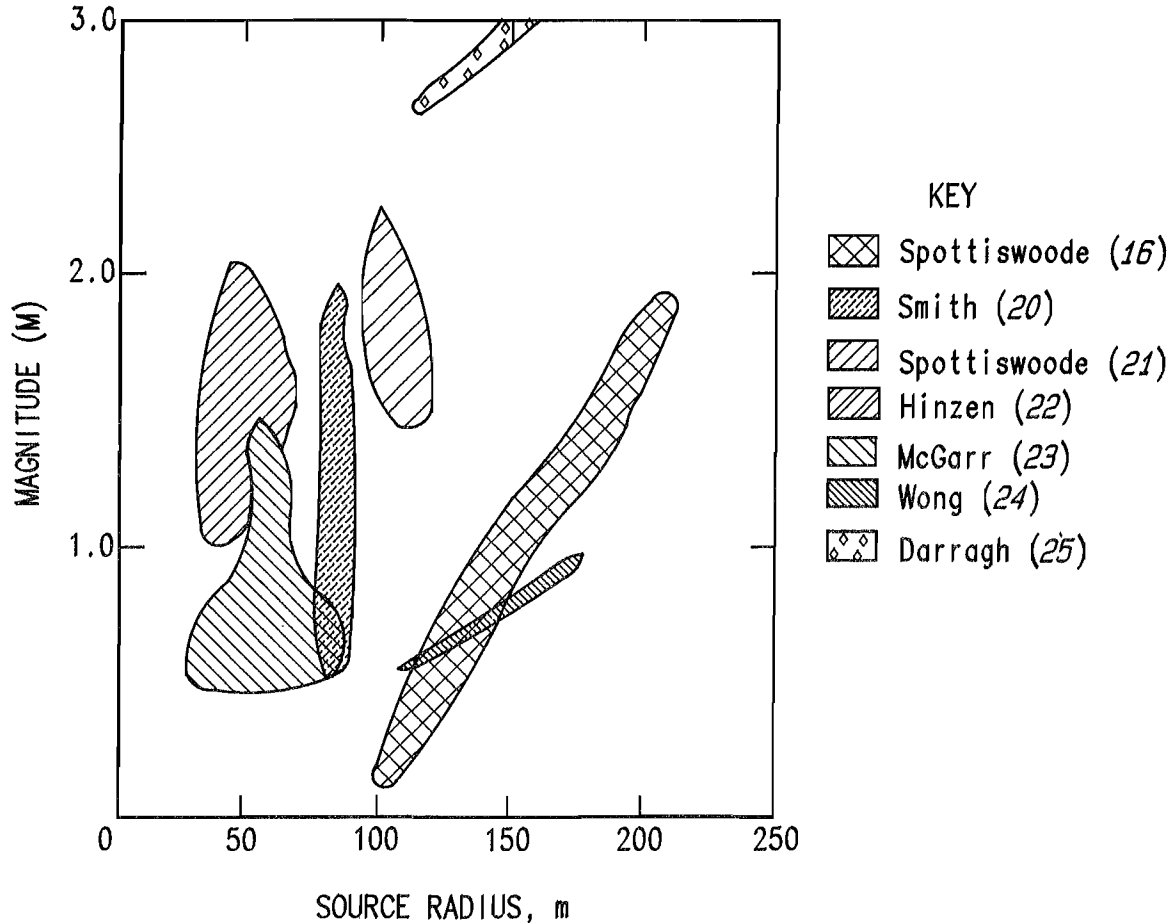


Figure 13.—Estimates of characteristic source dimensions based on dislocation shear-slip model of failure. Data are from references 16 and 20-25.

## SUMMARY

Seismicity induced by deep hard-rock mining in the Coeur d'Alene district of northern Idaho was recorded over a recent 20-month observation period and analyzed for its salient characteristics. These characteristics include seismic magnitude, time of occurrence, location, and relation to rock bursting and production blasting. In addition, several methods were used to estimate seismic source volumes and characteristic rupture dimensions associated with rock bursting.

Estimated magnitudes of the located seismicity range from -0.5 to 2.9. The  $b$  value, or slope of the logarithm of the number of seismic events with magnitude greater than  $M$  versus  $M$ , is estimated to be 0.5 for the approximately 150 events occurring throughout the mine. Approximately

60 pct of the seismic events with magnitudes greater than -0.5 and 75 pct of damaging rock bursts occurred within 45 min of production blasting. Seismic magnitudes of damaging rock bursts range from -0.5 to 2.9, with less damaging minor face bursts as small as -1.1. Estimates of rupture diameters associated with these rock bursts range from 3 to 300 m for  $M = -1.1$  to 2.9, respectively. These distances approximately correspond to the dimensions associated with the working face and with interstope and intervein dimensions. These observations suggest that, in addition to the existing quasi-static stress interaction between stopes and/or veins, there may also be a significant stress interaction due to static deformation accompanying larger mining-induced seismic events.

## REFERENCES

1. Steblay, B. J., T. Swendseid, and B. Brady. Innovative Microseismic Rock Burst Monitoring System. *Rockbursts and Seismicity in Mines (Proc. 2d Int. Symp. Rockbursts and Seismicity in Mines, Minneapolis, MN, June 8-10, 1988)*. Balkema, 1990, pp. 259-262.
2. Cook, N. G. W. The Seismic Location of Rockbursts. Paper in Proceedings of 5th U.S. National Symposium on Rock Mechanics. Pergamon, 1963, pp. 493-516.
3. Hodgson, K., and N. G. W. Cook. The Mechanism, Energy Content and Radiation Efficiency of Seismic Waves Generated by Rockbursts in Deep-Level Mining. *Dynamic Elastic Waves in Civil Engineering*. Wiley-Interscience, 1971, pp. 121-135.
4. McGarr, A., and G. A. Wiebols. Influence of Mine Geometry and Closure Volume on Seismicity in a Deep-Level Mine. *Int. J. Rock Mech. & Min. Sci.*, v. 14, 1977, pp. 139-145.
5. Lenhardt, W. A. Seismic Event Characteristics in a Deep Level Mining Environment. *Rock at Great Depth*. Balkema, v. 2, 1989, pp. 727-732.
6. \_\_\_\_\_. Damage Studies at a Deep Level African Gold Mine. *Rockbursts and Seismicity in Mines (Proc. 2d Int. Symp. Rockbursts and Seismicity in Mines, Minneapolis, MN, June 8-10, 1988)*. Balkema, 1990, pp. 391-394.
7. Blake, W., F. Leighton, and W. I. Duvall. Microseismic Techniques for Monitoring the Behavior of Rock Structures. *BuMines B 665*, 1974, 65 pp.
8. Gutenberg, B., and C. F. Richter. *Seismicity of the Earth*. Princeton Univ. Press, 1949, 273 pp.
9. Aki, K. A Probabilistic Synthesis of Precursory Phenomena. *Earthquake Prediction: An International Review*. Maurice Ewing Ser., v. 4, Am. Geophys. Union, 1981, pp. 566-574.
10. Richter, C. F. *Elementary Seismology*. Freeman, 1958, 768 pp.
11. Mogi, K. Magnitude Frequency Relation for Elastic Shocks Accompanying Fractures of Various Materials and Some Related Problems in Earthquakes. *Bull. Earthquake Res. Inst.*, v. 40, 1962, pp. 831-853.
12. Scholz, C. H. The Frequency-Magnitude Relation of Microfracturing in Rock and Its Relation to Earthquakes. *Bull. Seism. Soc. Am.*, v. 58, 1968, pp. 399-415.
13. Wyss, M. Towards a Physical Understanding of the Earthquake Frequency Distribution. *Geophys. J. R. Astron. Soc.*, v. 31, 1973, pp. 341-359.
14. Legge, N. B., and S. M. Spottiswoode. Fracturing and Microseismicity Ahead of a Deep Gold Mine Stope in the Pre-Remnant and Remnant Stages of Mining. Paper in Proceedings of the 6th International Congress on Rock Mechanics. Balkema, v. 2, 1987, pp. 1071-1077.
15. Gutenberg, B., and C. F. Richter. Magnitude and Energy of Earthquakes. *Ann. Geofis.*, v. 9, 1956, pp. 1-15.
16. Spottiswoode, S. M., and A. McGarr. Source Parameters of Tremors in a Deep-Level Gold Mine. *Bull. Seism. Soc. Am.*, v. 65, 1975, pp. 93-112.
17. Kasahara, K. *Earthquake Mechanics*. Cambridge Univ. Press, 1981, 248 pp.
18. Brune, J. N. Tectonic Stress and the Spectra of Seismic Shear Waves From Earthquakes. *J. Geophys. Res.*, v. 75, 1970, pp. 4997-5009.
19. \_\_\_\_\_. Correction. *J. Geophys. Res.*, v. 76, 1971, p. 5002.
20. Smith, R. B., P. L. Winkler, J. G. Anderson, and C. H. Scholz. Source Mechanisms of Microearthquakes Associated With Underground Mines in Eastern Utah. *Bull. Seism. Soc. Am.*, v. 64, 1974, pp. 1295-1317.
21. Spottiswoode, S. M. Source Mechanisms of Mine Tremors at Blyvooruitzicht Gold Mine. *Rockbursts and Seismicity in Mines (Proc. 1st Int. Congr. Rockbursts and Seismicity in Mines, Johannesburg, South Africa, 1982)*. S. African Inst. Min. and Metall., 1984, pp. 29-37.
22. Hinzen, K.-G. Source Parameters of Mine Tremors in the Eastern Part of the Ruhr-District (West Germany). *J. Geophys.*, v. 51, 1982, pp. 105-112.
23. McGarr, A., R. W. E. Green, and S. M. Spottiswoode. Strong Motion of Mine Tremors: Some Implications for Near-Source Ground Motion Parameters. *Bull. Seism. Soc. Am.*, v. 71, 1981, pp. 295-320.
24. Wong, I. G., J. R. Humphrey, J. A. Adams, and W. J. Silva. Observations of Mine Seismicity in the Eastern Wasatch Plateau, Utah, U.S.A.: A Possible Case of Implosional Failure. *Pure Appl. Geophys.*, v. 129, 1989, pp. 369-405.
25. Darragh, R. B., and B. A. Bolt. A Comment on the Statistical Regression Relation Between Earthquake Magnitude and Fault Rupture Length. *Bull. Seism. Soc. Am.*, v. 77, 1987, pp. 1479-1484.